Article

Not peer-reviewed version

Appendicular Skeleton of the Three-Toed Sloth (*Bradypus variegatus*) and Its Insights for Arboreal Adaptation in the Amazon Region

Michel Santos e Cunha , Rodrigo dos Santos Albuquerque , Daniel Furtado Perdigão , José Gonçalo Monteiro Campos , Vinicius Amanajas Celestino , Maria Eduarda Bastos Andrade Moutinho da Conceição , Thiago da Silva Cardoso , Thiago André Salvitti de Sá Rocha , Kayan da Cunha Rossy , Lucas Santos Carvalho , Luisa Pucci Bueno Borges , Sheyla Farhayldes Souza Domingues , Érika Renata Branco , Francisco Décio de Oliveira Monteiro * , Pedro Paulo Maia Teixeira

Posted Date: 30 May 2025

doi: 10.20944/preprints202505.2403.v1

Keywords: common sloth; tomography anatomy; suspensory locomotion; musculoskeletal adaptation; xenarthran morphology

 doi:10.20944/preprints202505.2403.v1

Article

Appendicular Skeleton of the Three-Toed Sloth (*Bradypus variegatus*) and Its Insights for Arboreal Adaptation in the Amazon Region

Michel Santos e Cunha [1], Rodrigo dos Santos Albuquerque [1], Daniel Furtado Perdigão [2], José Gonçalo Monteiro Campos [2], Vinicius Amanajas Celestino [2], Maria Eduarda Bastos Andrade Moutinho da Conceição [3], Thiago da Silva Cardoso [1], Thiago André Salvitti de Sá Rocha [3], Kayan da Cunha Rossy [1], Lucas Santos Carvalho [1], Luisa Pucci Bueno Borges [1], Sheyla Farhayldes Souza Domingues [1], Érika Renata Branco [4], Francisco Décio de Oliveira Monteiro [5,*] and Pedro Paulo Maia Teixeira [1]

[1] Institute of Veterinary Medicine, Pará Federal University, Belém 68740-970, Brazil
[2] Centro de Educação Profissional DNA, Ananindeua 67133-240, Brazil
[3] Department of Veterinary Clinic and Surgery, São Paulo State University, Jaboticabal, São Paulo, Brazil
[4] Institute of Animal Health and Production, Federal Rural University of the Amazon, Belém, Pará, Brazil
[5] Campus Araguatins of the Federal Institute of Education, Science, and Technology of Tocantins (IFTO), Araguatins 77950-000, Brazil
* Correspondence: deciomonteiro@ifto.edu.br

Abstract: The brown-throated three-toed sloth (Bradypus variegatus) exhibits unique suspensory locomotion that reflects specialized morphological adaptations to an arboreal lifestyle in the Amazon. This study aimed to describe the appendicular skeleton of B. variegatus using computed tomography (CT), providing detailed anatomical insights related to arboreal movement. CT scans were conducted on nine juvenile sloth cadavers, enabling three-dimensional visualization of thoracic and pelvic limb structures, including bones, joint configurations, and vestigial elements. Key findings include greater development of thoracic limbs compared to pelvic limbs, the absence of a clavicle suggesting vestigiality, fusion of carpal bones, and elongated claws—features that enhance limb strength, stability, and muscle attachment for suspensory behavior. Additionally, morphological traits such as a rounded acetabulum and laterally wide pubis support arboreal locomotion. The absence of a patella and variable ossification patterns also highlight evolutionary divergence and functional adaptations. These results contribute to our understanding of xenarthran morphology and offer valuable data for comparative anatomy, evolutionary biology, and conservation. Further studies are recommended to explore adult specimens and expand morphometric analyses.

Keywords: common sloth; tomography anatomy; suspensory locomotion; musculoskeletal adaptation; xenarthran morphology

1. Introduction

The arboreal lifestyle of the brown-throated sloth (Bradypus variegatus Schinz, 1825) found north of the Amazon and in northwestern Brazil, between the Negro and Branco rivers, differs from other quadrupedal mammals by its posture and obligatory suspensory locomotion [1,2]. General principles related to the mammalian quadrupedal locomotor ap-paratus such as Tamandua tetradactyla, Euphractus sexcinctus or Cebus apella also apply to modern sloths, such as suspension of the thorax between the forelimbs, body propulsion through rotation of the limbs on a proximal pivot, and the contribution of trunk move-ments [3–5].

The suspensive posture and locomotion of the sloth in arboreal habitat follows the consequences of a body in reverse gravity [6,7]. Anatomical particularities ease suspensory locomotion that requires variable coordination between the limbs, such as relatively rigid hook nails with great joint mobility in the proximal midcarpal and transverse tarsal, and also advantageous lever arms with a short scapula and a rounded thorax with a small di-ameter [8,9].

 doi:10.20944/preprints202505.2403.v1

Anatomical investigations may help to understand which are the morphological ad-aptations associated with a given lifestyle, as a suspensory arboreal one of the brown-throated sloth [10]. Diagnostic imaging methods can provide anatomic details that con-tribute to the knowledge of morphological adaptations and functions of organs and struc-tures in this species, enabling the comprehension of details through three-dimensional vi-sion when using computed tomography (CT) [11,12].

CT is used in several anatomical surveys because it allows morphological investiga-tion in live animals, especially when applied in studies related to organs and cavities that are difficult to access [13]. CT is used in veterinary medicine as an efficient and modern technique, as it allows the analysis of structures in three dimensions, distinguishing different types of tissues, contributing to the knowledge of morphology [14,15].

Research has been carried out on the morphological description of the skeletal system of several species, including the common sloth, which is essential to help understand what morphological adaptations are associated with a certain lifestyle [16]. Computed to-mography can be used in research on the anatomical approach to the skeletal system of wild animals, which may enable discoveries related to bone morphology and its influence on locomotion of these species [14]. The macroscopic morphology of the appendicular skeleton of Bradypus variegatus needs to be better elucidated by computed tomography. The description of sloth skeletal morphology with the aim of relating it to their locomotor adap-tations has already attracted the attention of scientists for many decades [2,17–19].

Computed tomography is widely used for anatomical studies, as it provides a mor-phological assessment of organic structures, including bones [20]. It is a versatile, fast, and efficient method used in various areas of medicine [21]. Another possibility of studies to understand bone morphology would be through dissection, however, it would be unfeasi-ble and limited to expand the bone structures of all cadavers.

Therefore, the alternative to understanding the morphological aspects of the appen-dicular skeleton of the brown-throated sloth was using CT, especially because this study is part of a comprehensive project that also investigates soft tissues, organs and cavities [12]. Therefore, the objective of this study is to elucidate the morphological adaptations of the appendicular skeleton in Bradypus variegatus using computed tomography (CT), with a focus on understanding of the bone structures facilitate arboreal locomotion and suspensory behavior in the Amazon region, such as limb proportions, joint configurations, and vestigial elements reflect volutionary adaptations to an arboreal lifestyle.

2. Materials and Methods

2.1. Animal Experimentation

The present study was conducted after the approval of the Animal Ethics and Welfare Committee of the Federal University of Pará (protocol No. 5943220321). The ethics principles of the European Commission for animal experiments involving animals (Directive 86/609EEC) were also followed.

In the present study, nine frozen corpses of Bradypus variegatus were used, 6 young males and 3 young females. These samples were frozen at -2°C to -10°C and came from hospital care at the Veterinary Hospital of the Federal University of Pará. They were sick animals, native to the Amazon region, close to the municipality of Castanhal, state of Pará, living wild and different populations, which were sent by an environmental agency of the Brazilian state, such as IBAMA-Instituto Brasileiro do Meio Ambeinte. These animals were classified as infants when they did not have a characteristic coat dimorphism and were less than 1.2 kg (<1,2 kg), and juvenile or young, when they presented a sexual dimorphism weighting more than 1.2 kg and less than 2.3 kg (1.2 kg–2.3 kg) according to Castro-Vásquez et al. [22].

2.2. Computed Tomography

The cadavers were initially defrosted in running water for approximately two hours. Then, they were placed in the dorsal decubitus on a rectangular foam pad, with extended forelimbs and extended hind pelvic limbs.

Images were obtained in the craniocaudal direction on a 16 channel helical tomographic device, Model Syngo CT 2009E (Siemens; Forchheim, Germany). The acquisition protocol was 110 kVp, 130 mA, scan time 62.66s and delay 3s, with a field of view (FoV) of 115 x 115 mm.

 doi:10.20944/preprints202505.2403.v1

The thickness of the slices was 5 mm sagittal with 1 mm multiplanar reconstruction (MPR) in the sagittal and dorsal planes. The acquired blocks of cuts were forwarded to CAD software (computer-aided design) for three-dimensional reconstruction in VR (volume rendering).

2.2. Evaluation of Bone Structure

After acquiring the images, descriptions and measurements of longitudinal and transverse anatomic characteristics of the thoracic and pelvic limbs of each specimen were made, using software tools. The adopted nomenclature was based on veterinaria nomina anatomica [23].

Measurements of bone length were made from longitudinal measurements between two points, taking into account the proximal and distal limits.

Regarding transverse measurements, they were obtained with the aim of identifying the mediolateral or craniocaudal diameter of the proximal and distal extremities and of the mid-diaphysis (Figure 1). The pelvic measurements were performed according to the methodology described by Eneroth et al. [24] (adapted), measuring the horizontal distance between: the distance between the two tubera coxae transverse diameter, the inner distance between the two acetabulum, the distance between the two lateral tubera ischiadica, the distance between the two medial tubera ischiadica. Right diagonal diameter, left diagonal diameter, sacropubic diameter, and horizontal distance from the ischial spines in the dorsal region were included.

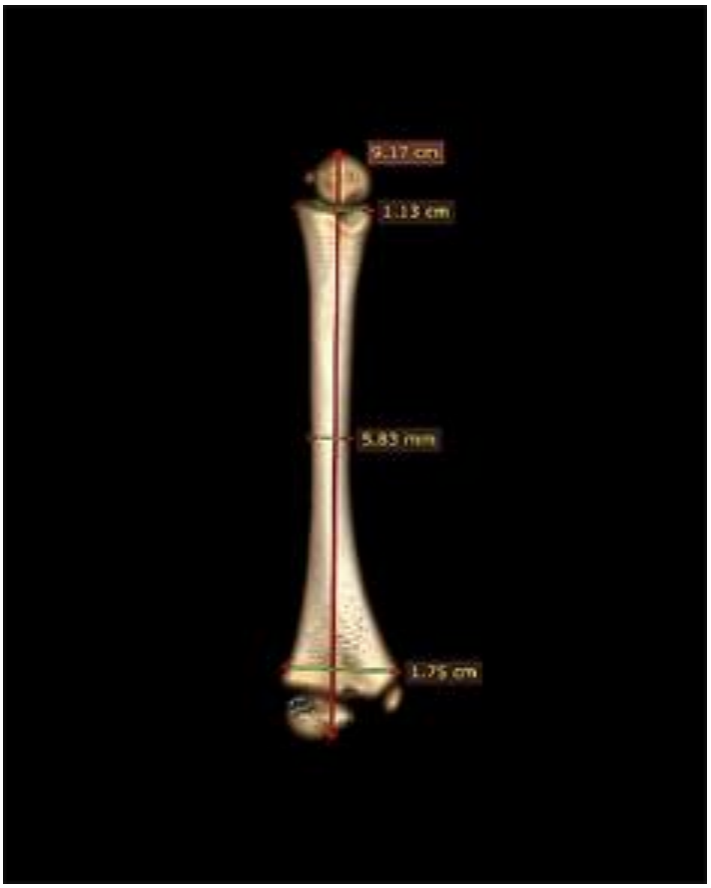

Figure 1. Tomographic image of *Bradypus veriegatus* humerus with cranial view. Method of gauging bone structures of the species. Note the longitudinal measurement from the caput humeri (most proximal point of the bone) to the epicondylus medialis (most distal point of the bone). The diameters of the proximal and distal metaphyses, as well as the diaphyseal bone isthmus, were also measured.

In the ventral region of the pelvis, the horizontal distance was measured between the anterosuperior crista iliaca was measured; horizontal distance between the corpus ossis ilii in its distal third; horizontal distance between the tuberculum pubicum ventrale in the pubic symphysis and the horizontal distance between the tuber ischiadicum (Figure 2A), while in the dorsal region, the horizontal distance of the spina ischiadica was also measured (Figure 2B).

 doi:10.20944/preprints202505.2403.v1

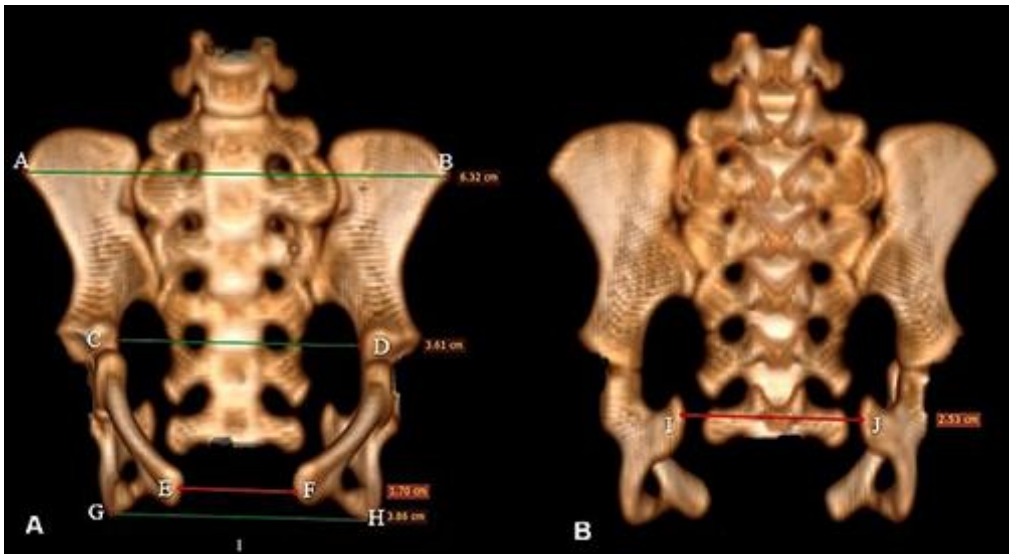

Figure 2. Tomographic image of the pelvis of *Bradypus variegatus* in ventral view **(A)** and dorsal view **(B)**. Note pelvimetry through horizontal measurements in the ventral region that were performed between the crista iliaca (green line between the points AB), between the caudal portion of the corpus ossis ilii (green line between the points CD), between the pubicum pubicum dorsale (red line between the EF points) and between the tuber ischii (green line between the points GH). The dorsal region was performed between the spina ischiadica (red line between the IJ points).

Morphometric analysis was not the subject of study, although some measurements were measured for morphological description. Furthermore, there was great variation in the size of the animals, which compromises the reliability of the measurements. Data were obtained based on the morphological descriptions of the collected samples, obtaining qualitative data.

3. Results

3.1. Forelimb

The scapula was described as a flat bone, proximal to the trunk, and the caudal, cranial, and dorsal margins. The dorsal margin of the scapula is convex and the ventral margin presents a concavity that strays away from the midline. Regarding the cranial and caudal angle, they were rounded (Figure 3A). The incisura scapulae and the coracoideus process are located cranioventral (Figure 3B).

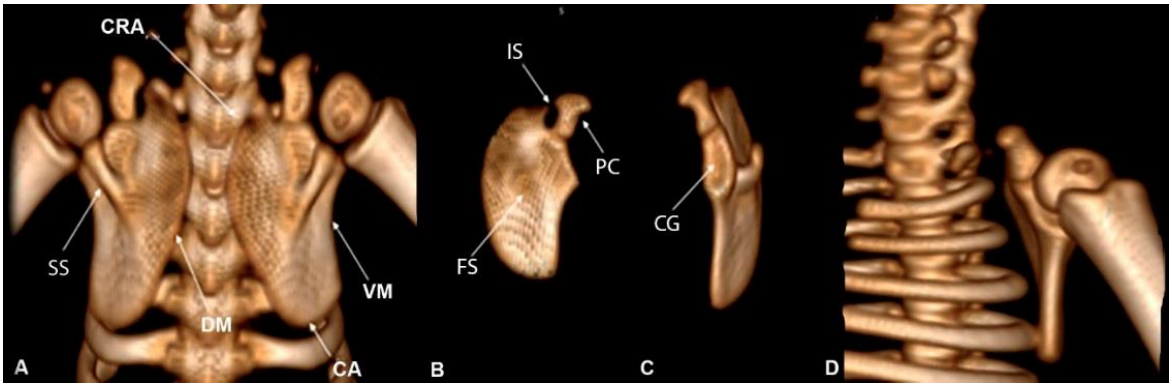

Figure 3. Computed tomography image in *Bradypus variegatus*: **(A)** dorsal view of the scapula showing the following anatomical structures: cranial angle (CRA), caudal angle (CA), spina scapulae (SS), dorsal margin (DM), ventral margin (VM). **(B)** Midcaudal view showing Incisura scapulae (IS), fossa supraspinata (FS), and process coracoideus (PC). **(C)** Cranial view, cavitas glenoidalis (CG). **(D)** Ventral view showing the absence of the acromion-clavicular joint.

Concerning the scapulae, the cavitas glenoidalis was observed cranially, which has a joint surface facing the ventral margin (Figure 3C). Dorsally there was a bone prominence that projected from the mid-diaphysis, laterocranially, to the cavitas glenoidalis, called the spina scapulae, which divides the supraspinata fossa and the fossa infraspinata, the infra being more elongated than the supra

 doi:10.20944/preprints202505.2403.v1

(Figure 3A). On the medial surface, the shallow subscapular fossa huged the rib cage. On the cranial portion, the presence of the acromion-clavicular joint was not observed (Figure 3D).

The humerus was characterized as a long cylindrical bone with a distance between the proximal and distal ends of 9.17 cm. The diameter of the diaphyseal isthmus was 5.83 mm, the proximal metaphysis was 1.13 cm, and the distal was 1.75 cm (Figure 4A). On the cranial surface of the proximal epiphysis is the caput humeri, which presents a slightly rounded ventral region, articulating with the cavitas glenoidalis of the scapulae, as well as the lesser and greater tubercles (scapulohumeral joint). The distal epiphysis in the craniocaudal direction is flat and it was possible to visualize the lateral and medial epicondylus. Two structures were also visualized: one medial and the other lateral, suggesting the trochlea and capitulum humeri (Figure 4B). A depression was observed at the edge of the proximal epiphysis at the height of the collum humeri in the dorsal region of the humerus. In the distal epiphysis, there is a bone depression located in the medial region of the humerus, suggesting that it is the fossa olecrani and the absence of the foramen supratrochleare (Figure 4A).

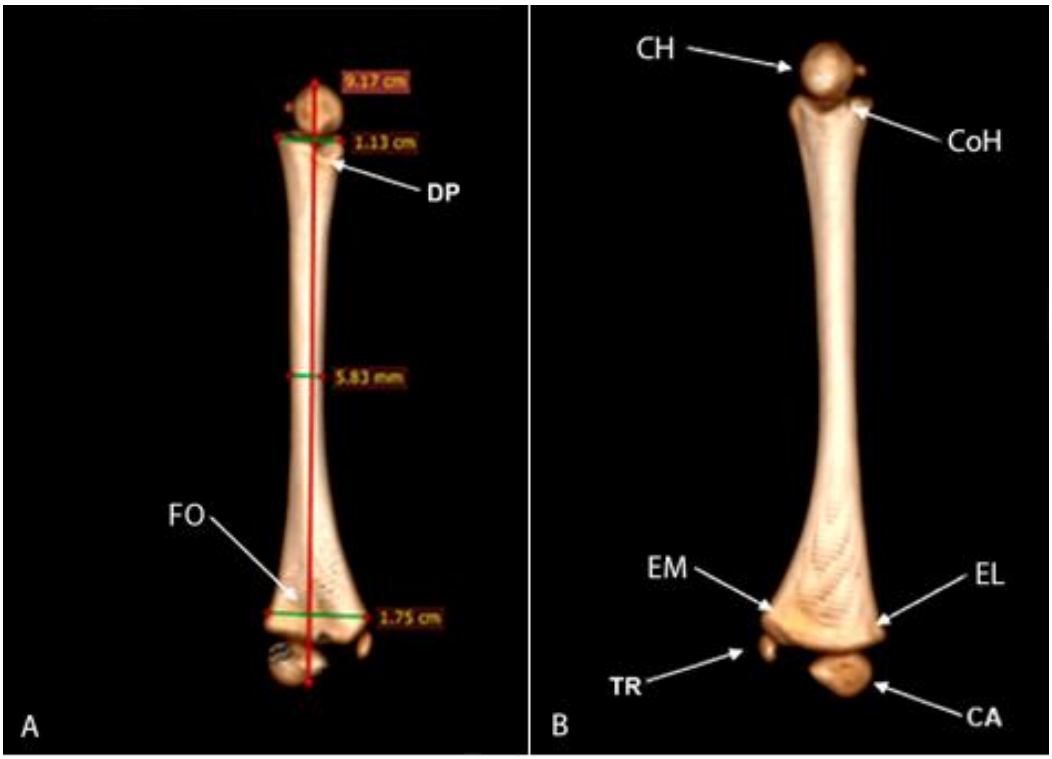

Figure 4. Computed tomography image of the humerus: caudal view of the humerus. **(A)** Measurements of the humerus, depression (DP), and fossa olecrani (FO). **(B)** Cranial view of humerus B, caput humeri (CH), collum humeri (CoH), medial epidondylus (EM), epicondylus lateralis (EL), trochlea (TR), capitulum (CA).

The thoracic limbs is composed of the radius and ulna, which presents a curvature and an interosseous space that completely separates them. The radius is a long and slightly curved bone. In the proximal region, it articulates with the humerus (epycondilus medialis and articulatio cubiti) and distally with the carpus (articulatio radioulnaris).

The radius length was 7.07 cm. The mid-diaphysis diameter was 4.63 mm and the mediolateral width of the proximal and distal epiphyses was 7.41 mm and 1.11 cm, respectively (Figure 5A).

 doi:10.20944/preprints202505.2403.v1

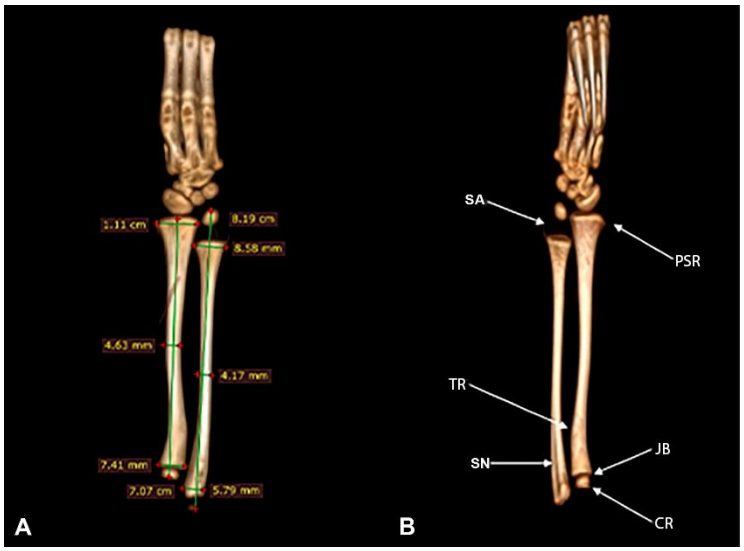

Figure 5. Computed tomography image of radius and ulna of *Bradypus variegatus*. **(A)** Dorsal view, measurements of the radius and ulna. **(B)** Palmar view, caput radii (CR), joint border (JB), tuberositas radii (TR), processus styloideus radii (PSR), shallow notch (SN), spacing area (SA).

In the proximal epiphysis, it was possible to see caput radii with a rounded appearance and its flat joint edge. In the proximal diaphysis, a medial curvature was visualized, which formed a small bony prominence called the tuberositas radii. Distally, near the carpi articulatio in the medial region, the styloideus process was observed (Figure 5B).

The ulna is located laterally in the forearm and attaches to the radius and humerus at its proximal extremity and to the radius at its distal extremity. This bone had a length of 8.19 cm between the epiphyses (from the styloid process of the olecranon to the ulnar axis) and a diameter of the mediolateral diaphysis of 4.17 mm. In its proximal and distal epiphyses, it had a mediolateral diameter of 5.79 and 8.58 mm, respectively (Figure 5A). Cranially, in the proximal epiphysis, a discreet bony protuberance was observed, followed by a slight shallow notch. In the proximal diaphysis, on its medial face, the presence of a groove was identified along the bone surface. The distal epiphysis was found to be substantially displaced from the ulnar metaphysis. The cartilaginous distal ulnar epiphysis is surprisingly long (Figure 5B).

However, in the caudal region, the structures described were observed with the absence of the sulcus on the proximal surface.

Five ossa carpi were identified, diffusely arranged, sliding freely between their joint surfaces, with the fifth carpal bone with the largest dimension fused directly to the base of the metacarpals (Figure 6A).

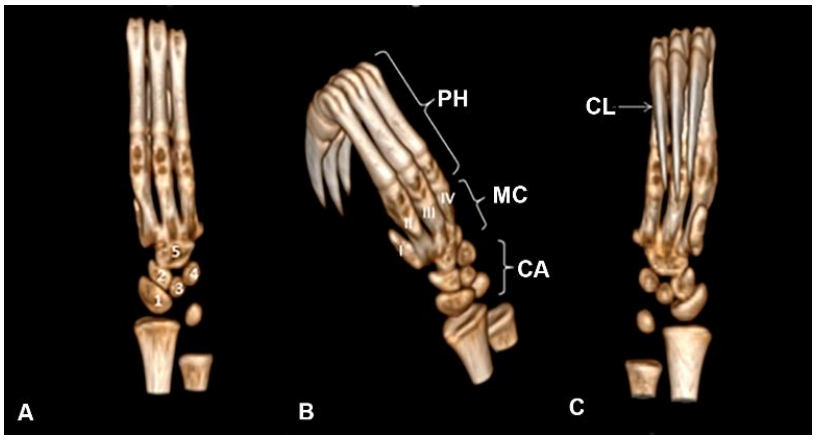

Figure 6. Computed tomography image in *Bradypus variegatus*. **(A)** Dorsal view with the bones of the carpus numbered 1, 2, 3, 4, and 5. **(B)** Oblique view, oss carpi (CA), ossa metacarpalia (MC) I-V, and phalanges (PH). **(C)** Ventral view (palmar), claw (CL).

 doi:10.20944/preprints202505.2403.v1

The presence of bone metacarpalia was observed with the absence of space in the articulatio metacarpophalangeae and with a first carpal bone with a reduction in dimension fused directly to the base of the metacarpals (Figure 6B). Phalanges comprise a total of nine structures, differing in the following: proximal, middle, and distal, with the middle relatively larger. The presence of long claws directly connected to the distal phalanges is highlighted (Figure 6C).

3.2. Pelvic Limb

The femur presents the diaphysis with a slight curve in the medial direction. The proximal epiphyses, as well as the distal ones, present discontinuity between the connection with the diaphysis, which is the area of the metaphysis. The diaphysis is compact with a mediolateral diameter of 7.51mm, with a distance between its epiphyses of 5.87 cm and a width in the proximal and distal thirds of 1.21 cm and 1.60 cm, respectively (Figure 7A).

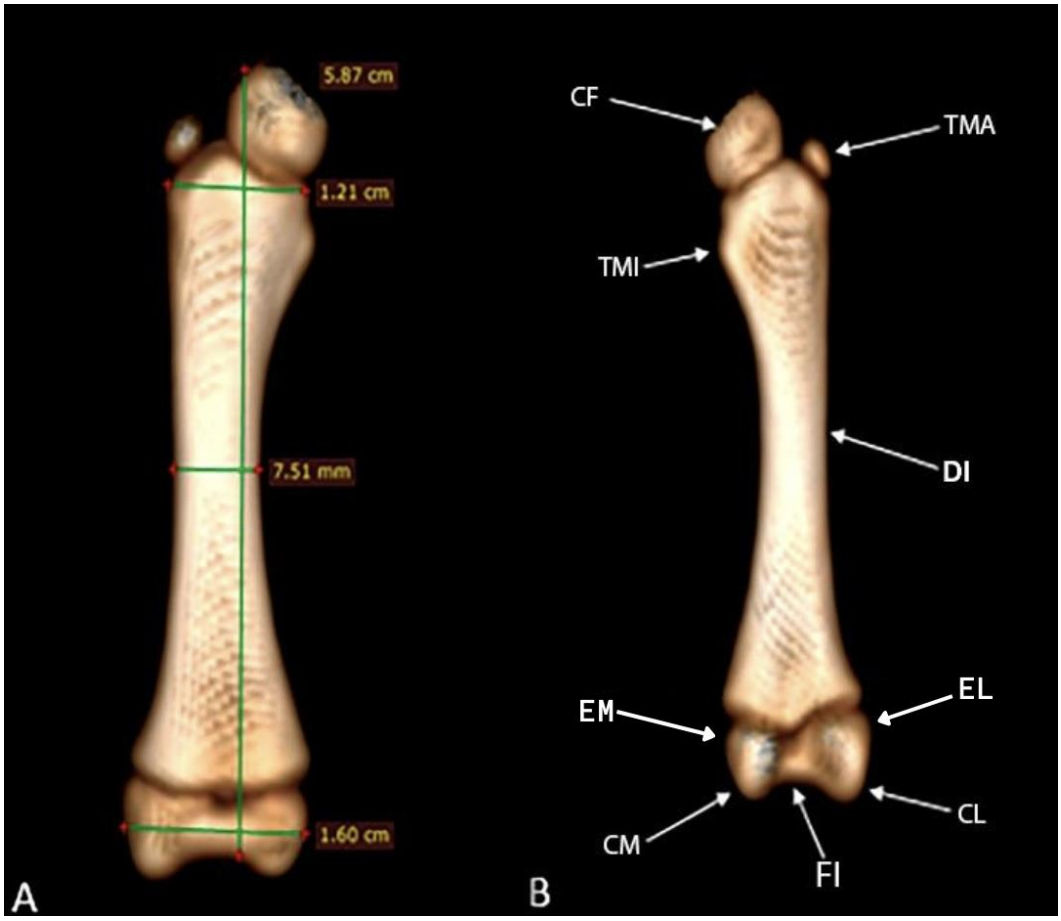

Figure 7. Computed tomography image of the femur of Bradypus variegatus: **(A)** Dorsal view, femur measurements. **(B)** Caudal view, caput ossis femoris (CF), trochanter major (TMA), trochanter minor (TMI), diaphysis (DI), epicondylus lateralis (EL), epicondylus medialis (EM), condylus lateralis (CL), condylus medialis (CM), fossa intercondylaris (FI).

On the cranial surface of the proximal epiphysis, the femoris caput is circular in shape with a flattened surface. Laterally, the epiphysis of the trochanter major is observed lateral to the femoris caput, and the trochanter minor is present on the medial side below the femoris caput. In the distal femoral epiphysis, the medial and lateral femoral condyles and there respective epicondyles were observed, and between them, caudally, the intercondylaris fossa. In the femorotibial articulatio, no patella was observed (Figure 7B).

The tibia presents at its extremities articulations with the fibula, which constitutes the articulatio tibiofibularis proximalis and distalis, in addition to a line of metaphysis. It also had a total length of 5.48 cm. The diameter of the diaphyseal isthmus was 4.69 mm. The mediolateral width of the cranial and distal metaphysis was 11.5 and 9.48 mm, respectively (Figure 8A).

 doi:10.20944/preprints202505.2403.v1

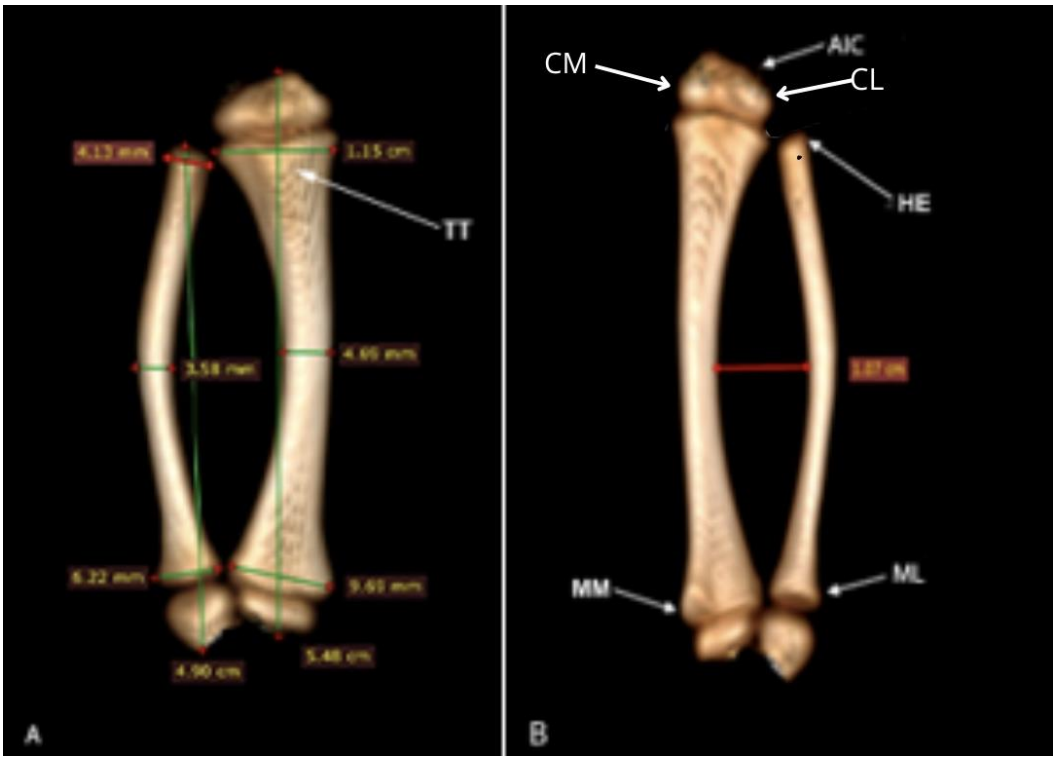

Figure 8. Computed tomography image in *Bradypus variegatus*: **(A)** Dorsal view, tuberositas tibiae (TT), tibia and fibula measurements. **(B)** Dorsal view, intercondylaris cranialis (AIC), condylus lateralis (CL), condylus medialis (CM), head (HE), malleolus lateralis (ML), malleolus medialis (MM).

It was possible to identify in the tibia, in its proximal cranial portion, the presence of a rough, irregular appearance and a homogeneous distribution on the side that is in contact with the metaphysis. More distally, it has a triangular shape, showing the tuberositas tibiae (Figure 8A), which corresponds to an area centered on the cranial surface and with a small protrusion that projects in the opposite direction to its central axis. The condylus medialis and the condylus lateralis also stand out as prominent structures that oppose each other (Figure 8B).

Distally from the tibia, the malleolus medialis was observed to be a structure without extensions that differentiate it from the area that opposes it. We could also observe the existence of a flat bone structure with irregular edges and a homogeneous distribution on the face that is in contact with the metaphysis area.

The fibula had length of 4.90 cm. The thickness of the mid-diaphysis was 3.58 mm, the proximal epiphysis was 4.13 cm and the distal 6.22 cm (Figure 8A). A rounded head with a smooth surface was identified in the proximal epiphysis. In the distal epiphysis, it was possible to observe the malleolus lateralis as a structure without extensions that differentiates it from the area that opposes it (Figure 8B). An oval bone structure with irregular edges and homogeneous distribution was observed on the face that is in contact with the metaphysis area.

3.3. Extremities of the Pelvic Limb

The set of ossa tarsi consists of a total of five bones with discrete joint spaces. In relation to the talus, it is the most proximal bone among them; it projects from the median to the medial plane and articulates laterally with the fibula and medially with the tibia, presenting a smooth surface in the cranial direction. Distally it articulates with the calcaneus navicular (Figure 9A).

 doi:10.20944/preprints202505.2403.v1

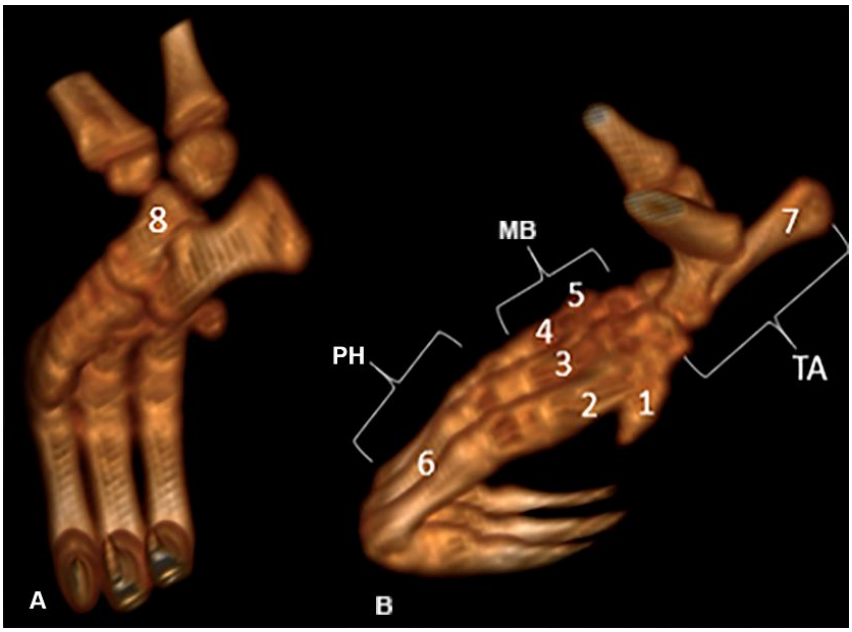

Figure 9. Computed tomography image of the distal extremity of the pelvic member of *Bradypus variegatus*: **(A)** Plantar oblique view, showing the talus (8); **(B)** dorsal oblique view, tarsus (TA), calcaneus (7), numbers 1,2,3,4,5 correspond to ossa metatarsalia I-V (MB), and 6, to the phalanges (PH).

The calcaneus is a laterally located bone of irregular dimensions laterally located with a prominent projection facing the caudal portion. It is possible to identify the articulation with the talus, which generates the articulatio talocalcanea, in addition to a concavity facing its ventral surface (Figure 9B).

Navicular is a medial bone without codominance between its linear dimensions. It articulates caudally to the talus, forming the talocalcaneonavicularis, and on its distal surface it communicates with one of the metatarsal bones, forming the tarsal-metatarsal joint.

A set of three fused cuneiform bones, located medially, was visualized, formed by fusion of bone pieces with a rough appearance that articulate to the metatarsals (Figure 9B).

The cuboideum is a laterally located bone identified cranial to the calcaneus and distal to the metatarsal.

The presence of ossa metatarsalia I-V was observed, with the first and fifth having proportionately smaller dimensions compared to the others. In the first metatarsal, it was possible to observe a structure with a conical aspect and a medial location. In the fifth metatarsal, a bone structure with an insinuation facing the lateral portion, articulating with the cuboideum and with the metatarsal was identified (Figure 9B).

The phalanges constitute a total of nine bones arranged, respectively, in the proximal phalanx,, the media phalanx and the phalanx distalis, with the second being relatively larger. Furthermore, the presence of elongated claws directly connected to the distal phalanges was also identified (Figure 9B).

3.4. Pelvis

The pelvis are a set of flat and irregular bones of equivalent length and width, with predominance over thickness. The pelvis is made up of a bony triad comprising the ilium, ischium, and pubis (Figure 10A). The ilium articulates with the sacrum to form the articulatio sacroiliaca.

 doi:10.20944/preprints202505.2403.v1

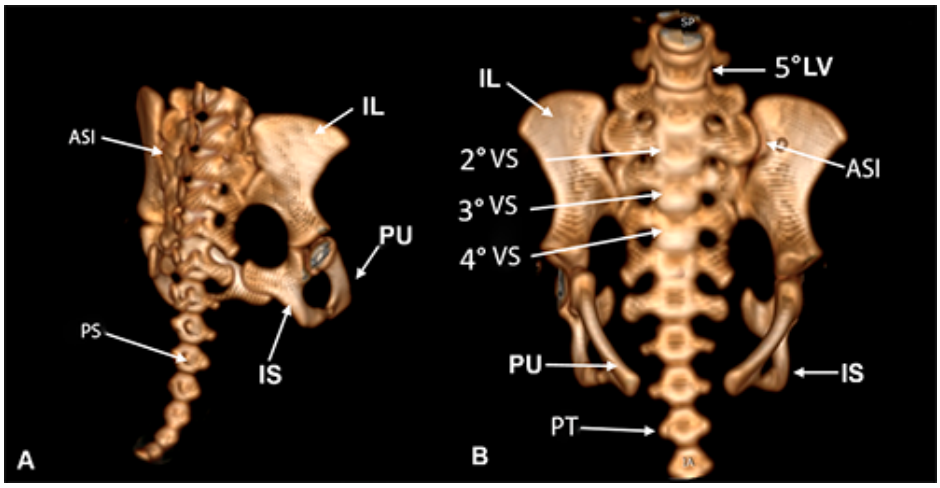

Figure 10. Pelvis in *Bradypus variegatus*. **(A)** Dorsal view, articulatio sacroiliaca (ASI), process spinosus (PS), ileum (IL), pubis (PU), ischium (IS). **(B)** Cranial view, ileum (IL), sacrales vertebrae (VS), pubis (PU), transversus (PT), lumbar vertebra (LV), articulatio sacroiliaca (ASI), ischium (IS).

The sacrum refers in its shape to an inverted pyramid with processus spinosus reduced in the caudal direction. This structure has six flat vertebral bodies, which articulate only the second, third, and fourth vertebrae with the ileum. The sacrum articulates cranially with the fifth lumbar vertebra and at the other end with the caudal vertebrae. These vertebrae present laterally the transverse processes and dorsally the spinous process, both poorly developed and reduced in the caudal direction (Figure 10B).

The acetabulum is formed by the union of the ischium, ilium, and pubis, with no connection between the latter two. The acetabulum has a curved and discontinuous shape with a smooth inner surface. The acetabulum region is interrupted in the ventral direction, causing the acetabuli of the fossa. This structure communicates with the foramen obturatum, which in this animal was characterized by a large oval-shaped orifice (Figure 11).

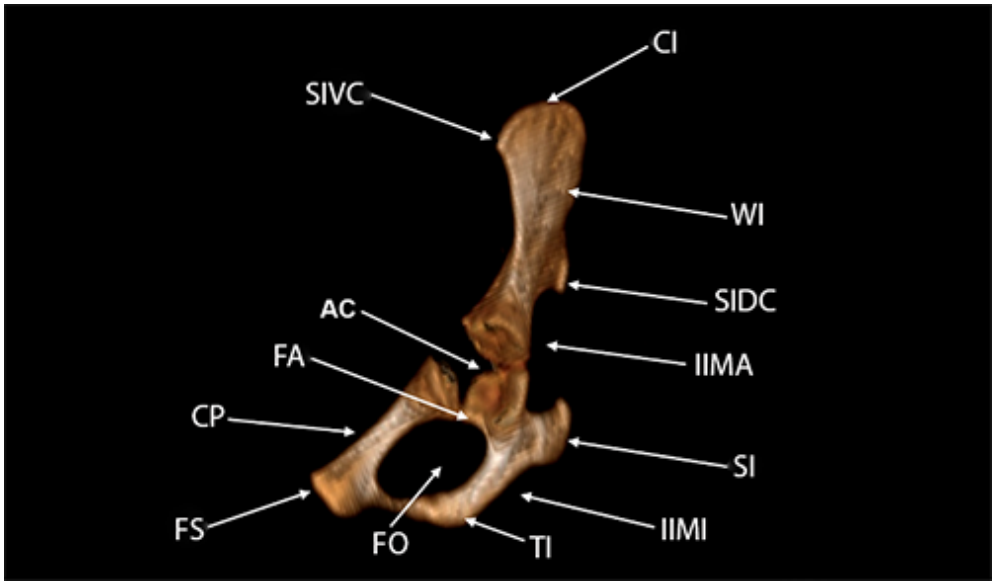

Figure 11. Computed tomography image of the pelvini ossa member of the common sloth (*Bradypus variegatus*). Left side view. Spina iliaca ventralis caudalis (SIVC), acetabulum (AC), fossa acetabuli (FA), corpus ossis pubis (CP), facies symphysialis (FS), foramen obturatum (FO), tuber ischiadicum (TI), incisura ischiadica minor (IIMI), spina ischiadica (SI), incisura ischiadica major (IIMA), spina iliaca dorsalis caudalis (SIDC), ala ossis ilii (WI), crista iliaca (CI).

The ilium is a flat and irregularly shaped bone, divided into two parts: corpus ossis ilii and ala ossis ilii, separated by the linea arcuata. The distance between the right and left crista iliaca was 6.32

 doi:10.20944/preprints202505.2403.v1

cm and 3.61 cm between their bodies in the distal third (Figure 2A). We did not check the ventralis cranial spina iliaca (Figure 2B).

The ischium showed a distance between the right and left tuber ischiadicum of 3.86 cm (Figure 2A). The cranial part of the body of the ischium fuses with the pubis and ilium. The ischii of ramus ossis connect to the ventral ramus of the pubis to form the ischiopubic ramus, which was thin, constituting the ventral limit of the foramen obturatum, which had an ellipsoid shape (Figure 12). At the dorsal margin of the ischium there is a pointed prominence facing cranially, called the spina ischiadica, which presented a dorsal distance of 2.53 cm (Figure 2B). This structure separates the greater from the incisura ischiadica minor, in which the form can be evidenced by its circular shape, more accentuated compared to the incisura ischiadica minor (Figure 12).

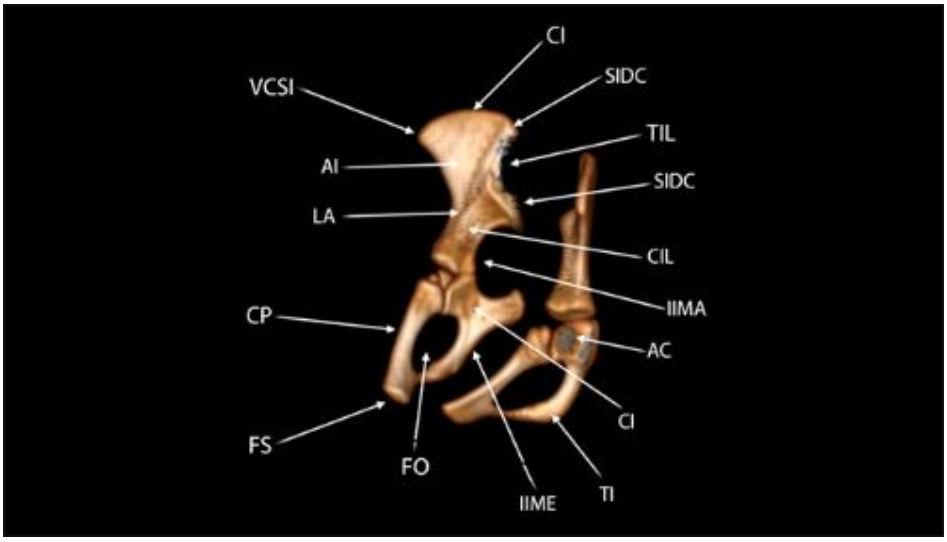

Figure 12. Computed tomography image of the pelvis of the common sloth (*Bradypus variegatus*). Side view, ventral-cranial spina iliaca (VCSI), ala ossis ilii (AI), linea arcuata (LA), corpus ossis pubis (CP), facies symphysialis (FS), foramen obturatum (FO), incisura ischiadica minor (IIME), tuber ischiadicum (TI), corpus ossis ischii (CI), acetabulum (AC), incisura ischiadica major (IIMA), corpus ossis ilii (CIL), spina iliaca dorsalis caudalis (SIDC), tuberositas iliaca (TIL), spina iliaca dorsalis cranialis (SIDC), crista ilaca (CI).

The pubis, being the smallest bone that forms the surface of the symphysialis of the pelvis, presents the right and left facies at the end of the pubic tuberculum, with 1.70 cm (Figure 2A).

4. Discussion

A The appendicular skeleton of *B. variegatus* presents is similar to *Choloepus didactylus* [25,26]. Furthermore, the larger pectoral limbs compared to the pelvic limbs, that includes the oblique scapular spine and more pronounced muscular development in these limbs with a small range of abduction are morphological aspects found in this species. The shape of bone morphological conformations, such as protuberances, concavities or discontinuities in the bone tissue, may be associated with movement and locomotion with a small range of limb abduction in these species [27,28].

The larger thoracic limbs compared to the pelvic limbs is a morphology of the bones that shows a characteristic of the species. It is a peculiar aspect of Bradypus, but having forelimbs (or thoracic limbs) longer than the hindlimbs (or pelvic limbs) is not a unique characteristic of this species. Mammals that perform suspensions and/or climbs generally present this characteristic (e.g., orangutans, gorillas) [29–31].

Phylogenetic and molecular data showed that Bradypus and Choloepus evolved independently, that is, they are not a monophyletic group. However, they are very similar in behavior and morphology, with an arboreal lifestyle and characteristic locomotion, the result of shared ancestry [32–34]. Thus, the musculoskeletal structure was adapted to perform suspensory posture and movements and to accomodate the reduced body muscle mass resulting from its diet based on leaves, sprouts and fruits [15,37].

There are discrepancies regarding the existence of a clavicle in *B. variegatus*. The presence of this bone is described in some studies and not in others. The clavicle has been described in young sloths and disappearing or being rudimentary in adults. The clavicle was not observed in this study. This

 doi:10.20944/preprints202505.2403.v1

allows us to advise that this structure cannot be used as a reference for the identification of this species, as there is individual variation; however, we reinforce the need for more extensive investigations to identify it in a larger population of individuals [37–39].

In studies carried out by Miller [2], Hautier et al. [37] and Nyakatura & Fischer [39] this variation in relation to the presence of the clavicle was reported. Miller [2] cites the *clavobrachialis* muscle of this species to strengthen the insertion of the deltoid and vestigial clavicle. When describing the forelimbs in sloths he reports that 1 and 5 metacarpals are vestigial, in Choloepus 1 and 4 metacarpals are vestigial. In view of what has been observed, we can consider this structure as a vestigial organ. In summary, the relationship between the sloth and the clavicle as a vestigial organ is related to the arboreal habits of these animals and their characteristic locomotion. The presence or absence of the clavicle may vary between individuals, but its functional importance has been reduced due to the adaptation to their natural environment [5,17–19].

The inconsistent pattern of ossification in *B. vagiegatus* justifies the incomplete bone fusion of some structures [40]. In the radius and ulna, interosseous spaces similar to those seen in humans were found, with spacing in the distal epiphysis of the ulna. Some structures may or may not be fused, however, the inconsistency of ossification in this species allows us to hypothesize a divergent line from the common being [41,42]. Bones that do not fully fused in adults are also quite common in marsupials, reflecting growth rates and life history strategies [43].

In the carpal region, five fused bones were identified, different from other species such as giant anteater and nonhuman primates. Fusion of these bones restricts wrist movements, and claws work as “pincers” adapted to hang and move in natural habitat, hypertrophying the musculature of the flexors in the finger along the forearm [44]. Therefore, we believe that since these animals spend most of their time hanging, they adapted and consequently there was a disproportion in these structures, since the pelvic limbs are used as a support point that functions as a “hook” in the tree trunks to increase the moment of displacement, facilitating the suspensory effect of the forelimbs [45].

The pelvic limbs are smaller than the pectoral limbs, indicating that they play a less important role in sloth locomotion than in typical arboreal quadrupeds. Therefore, the pelvic limb has a lower proportion than the humerus and the absence of a patella, which does not have a preponderant morphophysiological function in this species. The absence of the patella could just be due to the lack of ossification in this juvenile specimen. The lack of a patella in an adult is needed to confirm this observation. The tibia and fibula presented an irregular interosseous space that is articulated with the intercondylar notch, a finding similar to those found by Montilla-Rodríguez et al. [46] who described the triangular-shaped structure in the proximal epiphysis of the tibia.

The spinal and transverse processes of the caudal vertebrae can present changes in shape and development in *B. variegatus*, even in the same animal, depending on adaptation and behavior [47,48]. The pelvis in Xernathra is similar, the ischial spine turned cranially, with a thin ischial tuberosity, and the pubis with lateral amplitude, probably due to the fact that the sloth moves and fastens itself on the tree trunks. The rounded and deep acetabulum and the absence of the ventrocaudal iliac spine ensure the stability of the animal’s body [49,50].

5. Conclusions

Based on these results it was possible to describe in detail the bone structures of the limbs and pelvis of Bradypus variegatus, demonstrating the pronounced development of thoracic limbs compared to pelvic limbs, absence of a clavicle (suggesting vestigiality), and structural adapta-tions such as a rounded acetabulum and laterally wide pubis and fused carpal bones and elongated claws, which enhance stability and muscle attachment for arboreal mobility and life. These features align with the sloth’s unique suspensory lifestyle and reflect evolution-ary adaptations to its environment, contributing to broader discussions in evolutionary biology, biomechanics, and conservation. Limitations such as sample size and the absence of adult specimens warrant further investigation to deepen our understanding of these ad-aptations.

Author Contributions: Conceptualization, M.S.e.C., R.d.S.A. and P.P.M.T.; Methodology, J.G.M.C., F.D.d.O.M. and P.P.M.T.; Software, J.G.M.C., M.S.e.C. and F.D.d.O.M.; Validation, S.F.S.D., D.F.P., T.A.S.d.S.R. and P.P.M.T.; Formal Analysis, K.d.C.R., T.d.S.C. and L.P.B.B.; Investigation, T.d.S.C. and L.S.C.; Resources, L.P.B.B. and S.F.S.D.; Data Curation, K.d.C.R., F.D.d.O.M., D.F.P. and P.P.M.T.; Writing—Original Draft Preparation, M.S.e.C., F.D.d.O.M., L.P.B.B. and P.P.M.T.; Writing—Review and Editing, L.P.B.B., F.D.d.O.M., E.R.B and P.P.M.T.; Visualization, F.D.d.O.M., T.A.S.d.S.R., and P.P.M.T.; Supervision, S.F.S.D., V.A.C.; M.E.B.A.M.d.C and

 doi:10.20944/preprints202505.2403.v1

P.P.M.T.; Project Administration, S.F.S.D., E.R.B. and P.P.M.T. All authors have read and agreed to the published version of the manuscript.

Funding: This research received no external funding.

Institutional Review Board Statement: This study was carried out according to the recommendations of the National Council for Experimentation Control in Brazil (CONCEA). This research was approved by the Animal Ethics and Welfare Committee of the Federal University of Pará (protocol N ° 4848261017).

Acknowledgments: the authors gratefully thank the team of video surgery, obstetrics and reproduction group (VOR), the National Council for Scientific and Technological Development (CNPq, Brazil), the Coordination for the Improvement of Higher Education Personnel (CAPES, Brazil) and the Research and Postgraduate Pro-Rector of Pará Federal University (Propesp/UFPA) for financial support in the study.

Conflicts of Interest: The authors declare no conflicts of interest.

Abbreviations

CTComputed tomography

References

1. Moraes-Barros, N.d.; Giorgi, A.P., Silva, S.; Morgante, J.S. Reevaluation of the Geographical Distribution of *Bradypus tridactylus* Linnaeus, 1758 and *B. variegatus* Schinz, 1825. *Edentata,* **2010**, 11, 1, 53-61. https://doi.org/10.1896/020.011.0110.
2. Mendel, F.C. Use of hands and feet of three-toed sloths (*Bradypus variegatus*) during climbing and terrestrial locomotion. *J. Mammal.* **1985**, 66, 2, 359-366.
3. Granatosky, M.C.; Karantanis, N.E.; Rychlik, L.; Youlatos D. A suspensory way of life: Integrating locomotion, postures, limb movements, and forces in two-toed sloths Choloepus didactylus (Megalonychidae, Folivora, Pilosa). *J. Exp. Zool. A*. **2017**, 329, 10, 570-588. https://doi.org/10.1002/jez.2221.
4. Young, M.W.; McKamy, A.J.; Dickinson, E.; Yarbro, J.; Ragupathi, A.; Guru, N.; Avey-Arroyo, J.A.; Butcher, M.T.; Granatosky, MC. Three toes and three modes: Dynamics of terrestrial, suspensory, and vertical locomotion in brown-throated three-toed sloths (Bradypodidae, Xenarthra). *J. Exp. Zool. A*. **2023**, 339, 4, 383-397. https://doi.org/10.1002/jez.2684.
5. White, J.L. Indicators of locomotor habits in xenarthrans: Evidence for locomotor heterogeneity among fossil sloths, *J Vertebr Paleontol* **1993**, 13, 2, 230-242, https://doi.org/10.1080/02724634.1993.10011502
6. Buckland, W. On the adaptation of the structure of the sloths to their peculiar mode of Life. *Trans Linn Soc London* **1834**, 17, 1, 17–27. https://doi.org/10.1111/ j.1095-8339.1834.tb00015.x
7. Miller, R.A. Functional Adaptations in the Forelimb of the Sloths. *J. Mammal.* **1935**, 16, 1, 38–51. https://doi.org/10.2307/1374529. Accessed 25 Mar. 2024.
8. Mossor, A.M.; Young, J.W.; Butcher, M.T. Does a suspensory lifestyle result in increased tensile strength? Organ-level material properties of sloth limb bones. *J Exp Biol*. **2022**, 225, 5, jeb242866. https://doi.org/10.1242/jeb.242866.
9. Morgan, D.M.; Spainhower, K.B.; Mossor, A.M.; Avey-Arroyo, J.A.; Butcher, M.T. Muscle architectural properties indicate a primary role in support for the pelvic limb of three-toed sloths (*Bradypus variegatus*). *J. Anat.* **2023**, joa13884. https://doi.org/10.1111/joa.13884.
10. Montañez-Rivera, I.; Nyakatura, J.A.; Amson, E. Bone cortical compactness in 'tree sloths' reflects convergent evolution. *J. Anat.*, **2018**, 233, 5, 580-591. https://doi.org/10.1111/joa.12873.
11. Butcher, M.T.; Morgan, D.M.; Spainhower, K.B.; Thomas, D.R.; Chadwell BA, Avey-Arroyo JA, Kennedy SP, Cliffe RN. Myology of the pelvic limb of the brown-throated three-toed sloth (Bradypus variegatus). J. Anat. (2022) 240(6):1048-1074. https://doi.org/10.1111/joa.13626
12. Zehtabvar, O.; Masoudifard, M.; Rostami, A.; Akbarein, H.; Sereshke, A.H.A.; Khanamooeiashi, M.; Borgheie, F. CT anatomy of the lungs, bronchi, and trachea in the mature Guinea pig (*cavia porcellus*). *Vet. Med. Sci.* **2023**, 9, 3, 1179-1193. https://doi.org/10.1002/vms3.1131.
13. Cunha, M. S.; Albuquerque, R. dos S.; Campos, J.G.M.; Monteiro, F.D.O.; Rossy, K.C.; Cardoso, T. da S.; Carvalho, L.S.; Borges, L.P.B.; Domingues, S.F.S.; Thiesen, R.; Thiesen, R.M.C.; Teixeira, P. P.M. Computed Tomography Evaluation of Frozen or Glycerinated *Bradypus variegatus* Cadavers: A Comprehensive View with Emphasis on Anatomical Aspects. *Animals*. **2024**, 14, 3, 355. https://doi.org/10.3390/ani14030355.

 doi:10.20944/preprints202505.2403.v1

14. Mohamad, J.R.J.; González-Rodríguez, E.; Arencibia, A.; Déniz, S.; Carrascosa, C.; Encinoso, M. Anatomical Description of Loggerhead Turtle (*Caretta caretta*) and Green Iguana (*Iguana iguana*) Skull by Three-Dimensional Computed Tomography Reconstruction and Maximum Intensity Projection Images. *Animals*. 2023, 13, 4, 621. https://doi.org/10.3390/ani13040621.
15. Pereira, F.M.A.M.; Bete, S.B.S.; Inamassu, L.R.; Mamprim, M.J.; Schimming, B.C. Anatomy of the skull in the capybara (*Hydrochoerus hydrochaeris*) using radiography and 3D computed tomography. *Anat. Histol. Embryol.* **2020**, 49, 3, 317-324. https://doi.org/10.1111/ahe.12531
16. Li, Z.; Clarke, J.A. The Craniolingual Morphology of Waterfowl (Aves, Anseriformes) and Its Relationship with Feeding Mode Revealed Through Contrast-Enhanced X-Ray Computed Tomography and 2D Morphometrics. *Evol. Biol.* **2016**, 43, 12-25. https://doi.org/10.1007/s11692-015-9345-4.
17. Grand, T.I. Adaptations of tissue and limb to facilitate moving and feeding in arboreal folivores. In: Montgomery GG (ed) The Ecology of Arboreal Folivores. *Smithsonian Institution Press* **1978**, Washington, D. C., pp 231–241
18. Amson, E.; Nyakatura, J.A. The postcranial musculoskeletal system of xenarthrans: insights from over two centuries of research and future directions. *J. Mamm. Evol.* **2018**, 25, 459-484. https://doi.org/10.1007/s10914-017-9408-7
19. Spear, J.K.; Williams, S.A. Mosaic patterns of homoplasy accompany the parallel evolution of suspensory adaptations in the forelimb of tree sloths (Folivora: Xenarthra). *Zool J Linne Soc* **2020**, 193, 2, 445-463. https://doi.org/10.1093/zoolinnean/zlaa154
20. Pérez, S.; Encinoso, M.; Corbera, J.A.; Morales, M.; Arencibia, A.; González-Rodríguez, E.; Déniz, S.; Melián, C.; Suárez-Bonnet, A.; Jaber, J.R. Cranial Structure of Varanus komodoensis as Revealed by Computed-Tomographic Imaging. Animals 2021, 11, 1078. https://doi.org/10.3390/ani11041078
21. Withers, P.J., Bouman, C., Carmignato, S. et al. X-ray computed tomography. Nat Rev Methods Primers 1, 18 (2021). https://doi.org/10.1038/s43586-021-00015-4
22. Castro-Vásquez, L.; Meza, M; Plese, T; Moreno-Mora, S. Activity patterns, preference and use of floristic resources by *Bradypus variegatus* in a tropical dry forest fragment, Santa Catalina, Bolívar, Colombia. *Edentata*. **2010**, 11, 62-69. https://doi.org/10.1896/020.011.0111.
23. International Committee on veterinary gross anatomical nomenclature. Nomina Anatomica Veterinaria. 6th ed. Hannover, Ghent, Columbia, Rio de Janeiro: Editorial Committee, 2017. 178p.
24. Eneroth, A.; Linde-Forsberg, C; Uhlhorn, M; Hall, M. Radiographic pelvimetry for assessment of dystocia in bitches: a clinical study in two terrier breeds. *J Small Anim Pract*. **1999**, 40, 6, 257–264. https://doi.org/10.1111/j.1748-5827.1999.tb03076.x.
25. Gilmore, D.P.; Costa, C.P.; Duarte, D.P.F. Sloth biology: an update on their physiological ecology, behavior and role as vectors of arthropods and arboviruses. *Braz. J. Med. Biol. Res*. **2001**, 34, 1, 9-25. https://doi.org/10.1590/S0100-879X2001000100002
26. Presslee, S.; Slater, G.J.; Pujos, F. et al. Palaeoproteomics resolves sloth relationships. *Nat Ecol Evol* **2019**, 3, 1121–1130. https://doi.org/10.1038/s41559-019-0909-z
27. Püschel, T.A.; Sellers, W.I. Standing on the shoulders of apes: Analyzing the form and function of the hominoid scapula using geometric morphometrics and finite element analysis. *Am J Biol Anthropol.* **2016**, 159, 2, 325-341. https://doi.org/10.1002/ajpa.22882.
28. Nyakatura, J.A.; Stark, H. Aberrant back muscle function correlates with the intramuscular architecture of the dorsovertebral muscles in two-toed sloths. *Mamm. Biol.* **2015**, 80, 2, 114-121. https://doi.org/10.1016/j.mambio.2015.01.002.
29. Gebo, D.L. Climbing, brachiation, and terrestrial quadrupedalism: Historical precursors of hominid bipedalism. *Am. J. Phys. Anthropol.* **1996**, 101, 1, 55-92. https://doi.org/10.1002/(SICI)1096-8644(199609)101:1<55::AID-AJPA5>3.0.CO;2-C
30. Myatt, J.P.; Crompton, R.H.; Payne-Davis, R.C.; Vereecke, E.E.; Isler, K.; Savage, R.; D'Août, K.; Günther, M.M.; Thorpe, S.K.S. Functional adaptations in the forelimb muscles of non-human great apes. *J Anat* **2012**, 220, 1, 13-28. https://doi.org/10.1111/j.1469-7580.2011.01443.x

 doi:10.20944/preprints202505.2403.v1

31. Ruff, C.B.; Junno, J-A.; Burgess, M.L.; Canington, S.L.; Harper, C.; Mudakikwa, A.; McFarlin, S.C. Body proportions and environmental adaptation in gorillas. *Am. J. Phys. Anthropol*. **2022**, 177, 3, 501-529. https://doi.org/10.1002/ajpa.24443
32. Grass, A.D. Inferring differential behavior between giant ground sloth adults and juveniles through scapula morphology. *J Vertebr Paleontol*. **2019**, 39, 1. https://doi.org/10.1080/02724634.2019.1569018.
33. Gaudin, T.J. Phylogenetic relationships among sloths (Mammalia, Xenarthra, Tardigrada): the craniodental evidence. *Zool. J. Linn. Soc.* **2004**, 140, 255–305. https://doi.org/10.1111/j.1096-3642.2003.00100.x
34. Delsuc, F.; Kuch, M.; Gibb, G.C.; Karpinski, E.; Hackenberger, D.; Szpak, P.; Martínez, J.G.; Mead, J.I.; McDonald, H.G.; MacPhee, R.D.E.; Billet, G.; Hautier, L.; Poinar, H.N. Ancient Mitogenomes Reveal the Evolutionary History and Biogeography of Sloths. *Curr Biol*. **2019**, 29, 12, 2031-2042. https://doi.org/10.1016/j.cub.2019.05.043.
35. Casali, D.M.; Boscaini, A.; Gaudin, T.J.; Perini, F.A. Reassessing the phylogeny and divergence times of sloths (Mammalia: Pilosa: Folivora), exploring alternative morphological partitioning and dating models. *Zool. J. Linn. Soc.* **2022**, 196, 4, 1505–1551. https://doi.org/10.1093/zoolinnean/zlac041
36. Butcher, M.T.; Morgan, D.M.; Spainhower, K.B.; Thomas, D.R.; Chadwell, B.A.; Avey-Arroyo, J.A.; Kennedy, S.P.; Cliffe, R.N. Myology of the pelvic limb of the brown-throated three-toed sloth (Bradypus variegatus). *J. Anat.* **2022**, 240, 6, 1048-1074. https://doi.org/10.1111/joa.13626.
37. Hautier, L.; Weisbecker, V.; Sánchez-Villagra, M.R.; Goswami, A; Asher, R.J. Skeletal development in sloths and the evolution of mammalian vertebral patterning. *Biol*. **2010**, 107, 44, 18903-18908. https://doi.org/10.1073/pnas.1010335107.
38. Kaup, M.; Trull, S.; Hom, E.F.Y. On the move: sloths and their epibionts as model mobile ecosystems. *Biol. Rev*. **2021**, 96, 6, 2638-2660. https://doi.org/10.1111/brv.12773.
39. Nyakatura, J.A.; Fischer, M.S. Functional morphology and three-dimensional kinematics of the thoraco-lumbar region of the spine of the two-toed sloth. *J Exp Biol*. **2010**, 213, 4278-4290. https://doi.org/10.1242/jeb.047647.
40. Hautier, L.; Weisbecker, V.; Goswami, A.; Knight, F.; Kardjilov, N.; Asher, R.J. Skeletal ossification and sequence heterochrony in xenarthran evolution. *Evol. Dev*. **2011**, 13, 5, 460-476. https://doi.org/10.1111/j.1525-142X.2011.00503.x
41. Borges, N.C.; Nardotto, J.R.B.; Oliveira, R.S.L.; Rüncos, L.H.E.; Ribeiro, R.G.; Bogoevich, A.M. Anatomy description of cervical region and hyoid apparatus in living giant anteaters Myrmecophaga tridactyla Linnaeus, 1758. *Pesq. Vet. Bras.* **2017**, 37, 11, 1345-1351. https://doi.org/10.1590/s0100-736x2017001100025
42. Gavazzi, L.M.; Kjosness, K.M.; Reno, P.L. Ossification pattern of the unusual pisiform in two-toed (Choloepus) and three-toed sloths (Bradypus). *Anat. Rec*. **2021**, 305, 7, 1804-1819. https://doi.org/10.1002/ar.24832
43. Werning, S. Osteohistological differences between marsupials and placental mammals reflect both growth rates and life history strategies. *Integr. Comp. Biol.* **2013**, 53, E224-E224.
44. Olson, R.A.; Glenn, Z.D; Cliffe, R.N; Butcher, M.T. Architectural Properties of Sloth Forelimb Muscles (Pilosa: Bradypodidae). *J. Mamm. Evol., 2018*, 25, 573–588. https://doi.org/10.1007/s10914-017-9411-z
45. Spainhower, K.B.; Metz, A.K.; Yusuf, A.R.S.; Johnson, L.E.; Avey-Arroyo, J.A.; Butcher, M.T. Coming to grips with life upside down: How the type of myosin fibre and metabolic properties of sloth hindlimb muscles contribute to suspensory function. *J Comp Physiol*. **2021**, 191, 207–224. https://doi.org/10.1007/s00360-020-01325-x
46. Montilla-Rodrigues, M.A.; Blanco-Rodriguez, J.C.; Nastar-Ceballos R.N.; Munoz-Martinez, L.J. Descripción Anatómica de *Bradypus variegatus* em la Amazonia Colombiana (Estudio Preliminar). *Rev Fac Cienc Vet*. 2016, 57, 3-14.
47. Borges, N.C.; Cruz, V.S.; Fares, N.B.; Cardoso, J.R..; Bragato, N. Morphological evaluation of the thoracic, lumbar and sacral column of the giant anteater (*Myrmecophaga tridactyla* Linnaeus, 1758). *Pesq. Vet. Bras.* **2017**, 37, 4, 401-407. https://doi.org/10.1590/s0100-736x2017000400016
48. Cardoso, J.R.; Souza, P.R., Cruz, V.S.; Benetti, E.J.; Silva M.S.B., Moreira P.C.; Cardoso, A.A.L.; Martins, A.K.; Abreu, T.; Simões, K.; Guimarães, F.R. Anatomical study of the lumbosacral plexus of the Tamandua

 doi:10.20944/preprints202505.2403.v1

tetradactyla. *Arq. Bras. Med. Vet. Zootec*. **2013**, 65, 1720-1728. http://dx.doi.org/10.1590/S0102-09352013000600020

49. Granatosky, M.C.; Karantanis, N.E.; Rychlik L.; Youlatos, D. A suspensory way of life: Integrating locomotion, postures, limb movements, and forces in two-toed sloths *Choloepus didactylus* (Megalonychidae, Folivora, Pilosa). *J. Exp. Zool. A* **2017**, 329, 10, 570-588. https://doi.org/10.1002/jez.2221.
50. Gorvet, M.A.; Wakeling, J.M.; Morgan, D.M.; Segura, D.H.; Avey-Arroyo, J.; Butcher, M.T. Keep calm and hang on: EMG activation in the forelimb musculature of three-toed sloths (*Bradypus variegatus*). *J Exp Biol*, **2020**, 223, 14, jeb218370. https://doi.org/10.1242/jeb.218370